Investigations into nanofluids as direct solar radiation collectors

B.A.J. Rose[a]

H. Singh[a, *]

harjit.singh@brunel.ac.uk

N. Verma[a]

S. Tassou[a]

S. Suresh[b]

N. Anantharaman[b]

D. Mariotti[c]

P. Maguire[c]

[a]Institute of Energy Futures, Brunel University London, Uxbridge UB8 3PH, UK

[b]National Institute of Technology, Tiruchirappalli 620015, India

[c]Nanotechnology & Integrated Bio-Engineering Centre, Ulster University, Newtownabbey BT37 0QB, UK

[*]Corresponding author.

Abstract

Nanofluids that directly absorb solar radiation have been proposed as an alternative to selectively coated metallic receivers in solar thermal collectors. Given the expense of characterising a potential nanofluid experimentally methods for comparing nanofluids virtually are needed. This paper develops a computational wave optics model using COMSOL to simulate the absorption of nanoparticles suspended in a fluid for solar radiation (380–800 nm) and compares it to experimental results using reflectance and transmission spectrometry. It was concluded that while both yielded data with matching trends, the exact absorption of some fluids differed by up to 1 AU. Optical characteristics of nanofluids comprising ethylene glycol (melting point −12.99 °C and boiling point range 195–198 °C at 1013 h Pa) and graphene oxide (sheets size 5 nm × 19 nm × 19 nm, volume fraction 0.004–0.016%) have been experimentally measured. An optimum volume fraction of 0.012% of graphene oxide has been identified achieving a minimum reflectance and highest absorbance over the visible spectral range.

Keywords: Nanofluid; Direct solar absorption; Solar thermal collector; Optical absorption; Nanofluid stability; Wave optics model

1 Introduction

Nanofluids, suspensions of nanoparticles in liquids, have been the focus of recent interest for use as directly absorbing working fluids, due to their reported stability in suspension and the availability of materials from which they can be synthesised (Romasanta et al., 2011). Directly absorbing nanofluids offer many advantages over traditional surface absorbers: reduced thermal and radiative losses, potential for miniaturisation of solar concentrators and lower material costs (Toppin-Hector and Singh, 2013). The amount of solar radiation that a solar concentrator working fluid will directly absorb depends primarily on the type of fluid used and its solar absorption characteristics and the dimensions of the receiver tube (Gorji and Ranjbar, 2015; Toppin-Hector and Singh, 2013).

Extinction describes the reduction in the amount of radiation that is observed when any medium (gas or liquid or solid or a combination) is placed between a light source and a detector (Otanicar et al., 2009).

The attenuation of light intensity ($-dI_x$) as light passes through a layer of an absorbing medium is proportional to the intensity of light at the entrance of the medium layer (I_x) and the differential thickness of the layer (dx). Mathematically this relation can be expressed as (Maikala, 2010):

$$-dI_x = aI_x dx \quad \textbf{(1)}$$

~~Where~~where

a is the wavelength dependent absorption or extinction coefficient

Eq. (1) is popularly known as Bouguer-Lambert's law and in this equation '–' sign indicates a definite decrease in the intensity as light passes through any absorbing medium.

Previous studies have focussed on the scattering component using an adaptation of the Rayleigh approximation (Ladjevardi et al., 2013). However, the Rayleigh approximation only holds for particles that are spherical, are close in refractive index to the medium they are in, and are small in size relative to the wavelength (λ) such that $\ll \lambda/10$ (Kerker et al., 1978). Models based on the Rayleigh approximation will not be able to predict the optical properties of non-spherical particles such as graphene nanoparticles.

Taylor et al. (2011) took a Maxwell-Garnett effective medium approach to model the optical properties of nanofluids based on the optical properties of the fluid and the bulk materials of the nanoparticles (NPs). Their study has a serious drawback in that they did not consider any difference in the electrical permittivity between a nano scale particle and a macro scale sample of the same metal. They concluded that the Maxwell-Garnett effective medium approach did not correctly predict the extinction caused by nanoparticles in a fluid but did not expand on the reason nor suggest alternative methods.

Beer-Lambert's law relates the reduction in the intensity of light with the depth of medium layer as it passes through an absorbing medium of a specific concentration (C). Thus Eq. (1) can be expressed as Eq. (2) as follows:

$$-dI_x = aI_x C dx \quad \textbf{(2)}$$

Eq. (2) can be integrated over the thickness of the medium layer varying from $x = 0$ to $x = L$ to yield Beer's law (Maikala, 2010):

$$A = \log_{10}\frac{I_o}{I} \quad \textbf{(3)}$$

where

A is the absorbance of the absorbing medium

I_0 is the intensity of light that enters the medium

I is the intensity of light that leaves the medium layer of thickness L

Absorbance therefore can be easily linked with the depth of a medium. Beer-Lamberts law allows the absorbance for any path length through a medium to be calculated. This principle can be interpreted so that it is only necessary for a model to simulate the optical properties of a small volume of fluid to be useful for predicting the absorption of any volume. Currently the optical properties of each different fluid and particle combination must be measured experimentally to identify the ideal working fluid for a direct solar absorption application. If a computer model could be developed that is capable of identifying the most likely nanoparticle-fluid combinations, the process of designing a directly absorbing solar thermal concentrator would be greatly simplified.

1.1 Modelling approach

1.1.1 Raytracing

One of the simplest ways to model light absorption by objects is ray tracing. Ray tracing models light as being composed of several (how many depends on the precision of the model) infinitely narrow straight rays. A nanofluid would be simulated by a ray trace model as a series of opaque objects randomly distributed throughout a transparent medium (the population density and size of the objects is analogous to the volume fraction and size of nanoparticles). Rays are then passed through the virtual nanofluid and when they are incident on a nanoparticle they are considered to have been absorbed and propagate no further by simpler models. Once every incident ray has encountered a sphere and been absorbed, the distance travelled by the last ray to be absorbed and the number of rays used in the simulation can be used to estimate the depth of the fluid layer to cause full absorption of the solar radiation.

Ray trace models have the advantage of requiring relatively little information about the nanofluids and are based on simple geometric calculations to produce a result. However, they cannot accurately simulate the absorption of solar radiation by

nanofluids as nanoparticles are significantly smaller than the wavelength of solar radiation.

The uncertainty in the position of a photon makes it difficult to determine if a photon will be absorbed by a nanoparticle using a ray trace model. For a photon, it can be derived from the uncertainty principle expressed in Eq. (4).

$$\Delta x \geqslant \frac{\lambda}{4\pi} \tag{4}$$

where (Δx) is the uncertainty in position and (λ) is the wavelength.

For a photon of visible light uncertainty in the position is always greater than ~40 nm which is larger than the size of many nanoparticles considered for direct absorption (size ~15 to 30 nm). As such modelling light as rays at scales less than this is not a meaningful analogy (Novotny and Hecht, 2006). The wavelength of visible light could easily be around 10–25 times greater than the size of NPs. Thus, model assumption that light travels in straight lines and is only absorbed by particles on which it is directly incident is not valid (Bohren and Huffman, 1983).

As a result of these two shortcomings, a purely ray tracing based model only considers the interaction between particles and light directly incident on it. Such a model would either under- or over-estimate the optical absorption by a nanofluid. An alternative would therefore be to simulate the process using ray tracing only at scales where its assumptions are sensible and an alternative model to simulate the fluid properties at smaller scales.

1.1.2 Wave optics

While the Rayleigh approximation was originally derived geometrically it has been shown to be consistent with wave optics (Bohren and Huffman, 1983).

The interaction of electric and magnetic fields is described physically by Maxwell's, Eqs. (5)–(8).

$$\nabla \times \boldsymbol{E}(\boldsymbol{r},t) = -\frac{\partial \boldsymbol{B}(\boldsymbol{r},t)}{\partial t} \tag{5}$$

$$\nabla \times \boldsymbol{H}(\boldsymbol{r},t) = \frac{\partial \boldsymbol{D}(\boldsymbol{r},t)}{\partial t} + \boldsymbol{j}(\boldsymbol{r},t) \tag{6}$$

$$\nabla \cdot \boldsymbol{D}(\boldsymbol{r},t) = \rho(\boldsymbol{r},t) \tag{7}$$

$$\nabla \cdot \boldsymbol{B}(\boldsymbol{r},t) = 0 \tag{8}$$

~~Where~~ where (E) is the electric field; ($\boldsymbol{D}$) is the electric displacement; ($\boldsymbol{H}$) is the magnetic field; ($\boldsymbol{B}$) is the magnetic induction; (j) is the current density, (ρ) is the charge density, ($\nabla\times$) represents the curl of a vector and ($\nabla\cdot$) represents the divergence of the vector.

Light is therefore described by wave optics as an electromagnetic wave comprised of varying electric and magnetic fields orthogonal to each other and the direction of wave propagation.

In vacuum electromagnetic waves will continue to propagate indefinitely whereas in other mediums charges will be affected by the varying electrical and magnetic field which will diminish energy content of the wave as it passes through. In this way the electromagnetic wave is absorbed and its energy is transferred to the medium.

A medium's resistance to a change in electric field and magnetic field is given by the electrical permittivity (ε) and magnetic permeability (μ) respectively. These properties are more commonly represented in terms of the refractive index (n) (9).

$$n = \sqrt{\frac{\varepsilon}{\varepsilon_0}\frac{\mu}{\mu_0}} \tag{9}$$

where (ε_0) is the electrical permittivity of free space and (μ_0) is the magnetic permeability of free space.

In most circumstances, at speeds much less than the speed of light or intensities less than 10^{18} W/m^2, only the electric field and electrical permittivity need be considered (Peatross and Ware, 2011). The wave equation for the electric field in a medium with a refractive index (n) can be written as shown in Eq. (10).

$$\nabla^2 E - \frac{n^2}{c^2}\frac{\partial^2 E}{\partial t^2} = 0 \tag{10}$$

where (c) is the speed of light.

A wave optics model of a nanofluid can be built from the refractive indices of the nanoparticles and base fluid, particle size and particle distribution in the fluid. Such model can solve the wave equation for the electric field (and magnetic field, if necessary) at every point in the fluid.

In this study a wave optics model is developed to estimate the optical properties of nanofluids to aid in sizing the absorber tubes and selecting working fluids for directly absorbing solar concentrators. The results computed by the model are compared with those obtained experimentally.

2 Methodology

2.1 Wave optics model

The proposed model was constructed using the wave optics module of COMSOL Multiphysics. A 1 µm × 1 µm × 8 µm control volume, Fig. 1, was defined and given the electrical and optical properties of ethylene glycol. The control volume was large enough to avoid effects resulting from scales close to those of the wavelengths used (diffraction off the edges of the volume) and yet small enough to compute reasonably fast (around 1 h). The process of simulating the nanoparticles was still complex as the electrical permittivity of a material is governed by the states of charges (protons, electrons) in that material and the amount of the material (Podolskiy et al., 2002). The energy level in which a charge can exist is affected by the number of other charges in the material ~~(Koh et al., 2009)~~.

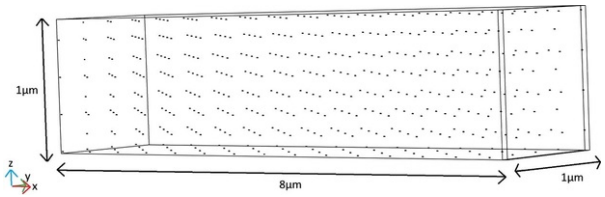

Fig. 1 The simulated control volume containing two offset nanoparticle arrays.

In bulk samples of material (other than near the edges) the number of surrounding charges approaches infinity (from the perspective of an individual charge). At the nanoscale, however, the number of other charges in a particle is far from infinity (maybe only a couple of thousand) therefore the states available for each individual charge will be different to a charge in a macroscale bulk sample of the same material. Clearly, such bulk measurements for electrical permittivity of a material cannot be used directly for nanoparticles.

This has been observed experimentally by Ni et al. (2007) who reported an apparent difference in refractive index between graphene and graphite of $0.6-0.2i$, graphite having a refractive index of $2.6–1.3i$ (Palik, 1998) and graphene $2.0–1.1i$. They attributed this difference to the nano scale of the graphene sheet's thickness.

Within the control volume two arrays were defined comprising identical 5 nm × 19 nm × 19 nm nanoparticles making up the equivalent of 0.1% of the simulated volume. These nanoparticles were assigned the complex refractive index of graphene from Ni et al. (2007). The surroundings were assigned the refractive index of ethylene glycol. The arrays were positioned off set from each other so the distance between each particle and a neighbouring particles was not the same, in all directions, see Fig. 1.

At one of the 1 × 1 µm faces of the volume a linearly polarised electric field with a power of 25 nW (equivalent to a solar radiation intensity of 1000 W/m^2 concentrated 25 times) was applied. The top, bottom and far end faces were assigned impedance boundary conditions while at the other two sides the curl of the magnetic field was set to zero. The model was then used to calculate the electric field at every point in the simulated volume as the electric field at one face was varied from 700 nm/428THz to 400 nm/750THz in steps of 25THz. The range covered, 700 nm/428THz to 400 nm/750THz, approximately encompasses the visible solar spectrum (380~~nm~~–800 nm).

2.2 Experimental investigations

To validate the predictions of the wave optics model experimentally, samples of nanofluids containing ethylene glycol and 5 nm × 19 nm × 19 nm size graphene oxide platelets were prepared via the two step method, where nanoparticles are prepared separately and then added to the base fluid using an ultrasound bath to ensure they are homogenously dispersed. The chosen volume fractions of 0.004%, 0.008%, 0.012%, 0.013%, 0.014% and 0.016% are those over which the absorption is expected to follow a linear trend and are below the critical concentration at which the nanoparticles start to bundle together.

2.2.1 Absorption

The absorption of each sample was measured over the spectrum range of 380–800 nm in steps of 1 nm using Perkin Elmer Lambda 650 S UV/VIS Spectrometer. The instrument was calibrated with a holmium oxide glass standard. A pure sample of ethylene glycol (melting point −12.99 °C and boiling point range 195–198 °C at 1013 h Pa) was used as the control. A spectrometer subjects a sample with radiation at a range of wavelengths and measures the intensity of each wavelength passing through it. The disadvantage of this method is that it is more sensitive to low absorbing materials as more radiation are transmitted through them to be measured.

2.2.2 Reflectance

While in the computerized model light enters fluid directly, in the experiment light must first pass through the walls of the fluids container. This will result in four points where the light may be reflected, at each boundary between the air and the container and at the boundaries between the container and the fluid. Any light reflected at these points will not pass through the fluid and will not reach the detector, however it will not have been absorbed by the fluid.

Additionally, light is also scattered within the fluid by the particles. The rationale for the development of the wave optics model was based on the assumption that extinction due to scattering would be low in comparison to extinction resulting from absorption for the nanofluids under investigation as the majority of light scattered within the fluid would still be absorbed before leaving the fluid.

The integrating sphere method is a standard way of measuring the light scattered and reflected by a sample. The instrument is comprised of a sphere, with an inside surface that scatters light evenly around the chamber. When a small part of the surface (referred to as a port) is replaced by a sample, any change in light levels measured by the detector is therefore the result of light scattered back into the chamber by the sample.

The reflectance resulting from the nanofluid samples was measured from 380 nm to 800 nm in steps of 1 nm using the same Lambda 650 S UV/VIS in integrating sphere mode. Each sample was placed over an open port and the reflectance was measured by the instrument. For comparison the reflectance of an empty cuvette, a pure sample of ethylene glycol, and the open port were also measured. The light lost by reflection could then be taken from absorbance measurement of each sample to calculate absorption of the fluid sample in isolation.

2.2.3 Stability

To ensure stability of synthesised nanofluids and to confirm repeatability of results, stability tests were carried out on each sample.

Stability is critical for nanofluids to be considered for their use as working fluid in direct solar absorber, if the nanoparticles segregate during periods that the solar concentrator plant is not in use the optical and thermal properties of the nanofluids could be radically altered. Precipitated particles may also block pipes and damage pumps.

To assess the ethylene glycol graphene oxide nanofluid's stability, the 0.008% sample (selected because its absorption had been previously shown to be in the mid-range of the instruments sensitivity) was left undisturbed in the spectrometer. The sample's absorption was measured after 1, 2, 3 and 24 h to determine the colloidal stability of the fluid over this period. A slight change in the absorption of the sample after 24 h may be expected as the sample was briefly removed to recalibrate the instrument.

3 Results

3.1 Modelling

The nanoparticles in the simulated volume were assigned the complex refractive indices of Graphene sheets 2.0–1.1i (Ni et al., 2007). The simulated volume with areas of high electric filed strength in red, low electric field strength in blue, is shown in Fig. 2.

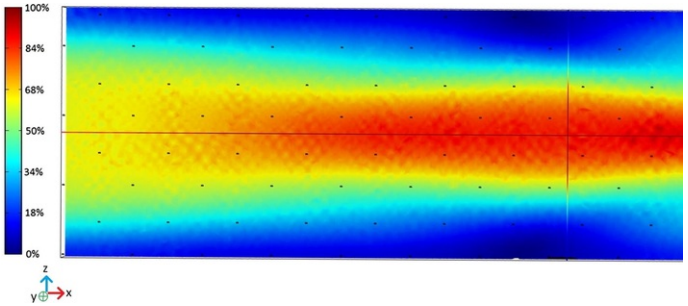

Fig. 2 Electric field strength in the simulated volume, the field enters at the right hand side; high electric field strength areas are shown in red and low electric field strength in blue. (For interpretation of the references to colour in this figure legend, the reader is referred to the we version of this article.)

Near the edges of the control volume the boundary conditions force the electric field to be close to zero, as a result smaller control volumes were not penetrated by the electric field. In Fig. 2 the volume has a cross section measuring 1 μm × 1 μm, which is sufficiently large for the electric field in the centre to propagate mostly unaffected by the boundaries. For each simulation the electric field strength along the x-axis passing through the geometric

centroid of the control volume is plotted in Fig. 3.

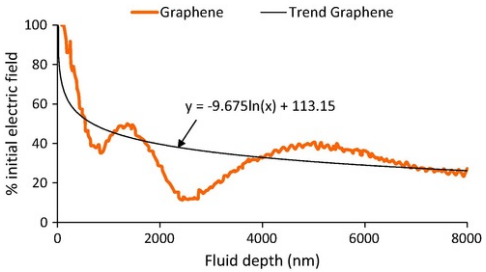

Fig. 3 Variation of electric field with depth on the central x-axis of the simulated control volume.

While there is substantial variation in the plots there is an overall trend for the field strength to reduce logarithmically with depth, as would be expected from Beer-Lamberts law, Eq. (2), as shown by the trend line. Initial investigations revealed that a larger and more regular variation resulted from the interaction of radiation with the regular array of nanoparticles; changing either the wavelength or the nanoparticles' arrangement in the array altered this trend. Fig. 3 also shows that the properties of the nanoparticles also affected the positions of peaks and troughs.

A smaller scale less regular variation seemed to be resulting from a combination of the mesh and particle shape, the corners of the cuboids had a particularly strong effect on the electric field (Fig. 4a), and can also be seen as a distinct checkered pattern visible in certain areas of Fig. 2. The checkered pattern did not appear for spherical nanoparticles in which case the electric field near particles varied less erratically as shown in Fig. 4b.

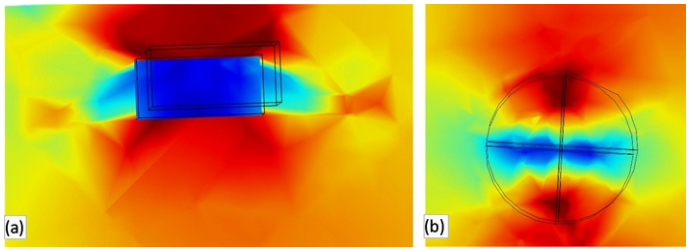

Fig. 4 Electric field strength around (a) a cuboid particle and (b) a spherical particle; red areas show a higher electric field strength and blue a low electric field strength. (For interpretation of the references to colour in this figure legend, the reader is referred to the web version of this article.)

The average values for absorbance in the range of 380–800 nm of 10 mm thick layer of nanofluids containing ethylene glycol with 0.004–0.016% volume fraction graphene nanoparticles were calculated to obtain the trend line shown Fig. 5. The absorbance of 0.016% was obtained from simulation results whilst for all other volume fractions the absorbance values were approximated from the graphene trend line (Fig. 3) assuming Beer-Lamberts law to be applicable. Also the test volume may have been too small (8 μm) to fully average the variations shown in Fig. 2 and Fig. 3.

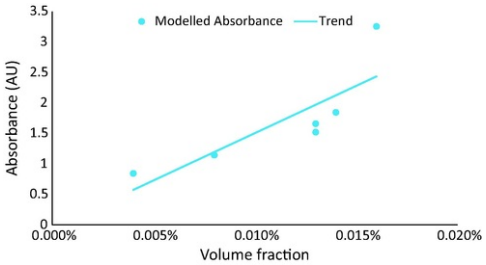

Fig. 5 Model predicted absorbance for ethylene glycol and graphene nanofluids.

3.2 Experimental results

Results of the computer modelling described in Section 3.1 and Fig. 3 confirmed that Beer-Lamberts law held for the nanofluid; the absorbance doubled when the length of the sample was doubled. This was also the case for volume fraction, when the volume fraction was doubled the absorbance proportionally increased.

3.2.1 Absorption

The absorption spectra of nanofluids measured experimentally are shown in Fig. 6.

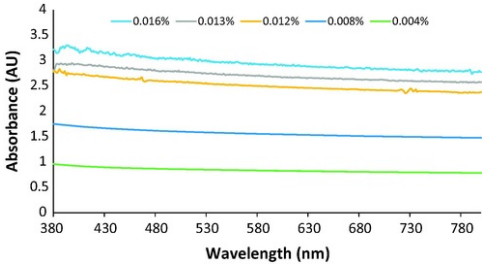

Fig. 6 Absorbance spectra of nanofluids with different volume fractions of graphene oxide.

As predicted by the model, the nanofluids were close to be equally absorbing over the full range of the spectrum. To compare the predictions of the model with the experimental measurements the average absorbance across the spectrum (380–800 nm) and volume fractions covered were calculated and plotted in Fig. 7. Error in measurement was observed to be ±7.5%.

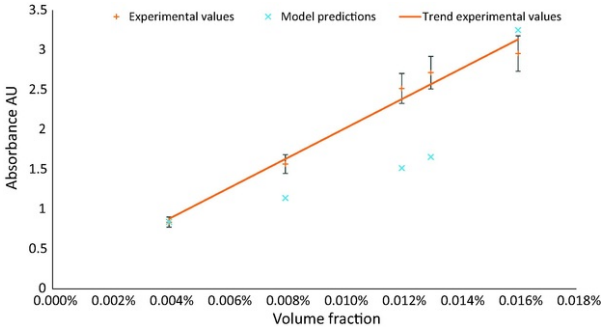

Fig. 7 Modelled and experimental average absorbance of nanofluids across the solar spectrum (380–800 nm).

As expected the experimental data points in Fig. 7 follow a linear relationship. While the absorbance for 0.004% and 0.016% volume fraction were close to those predicted by the model (Fig. 5) the intermediate volume fractions were found be up to 1AU higher than the predicted absorbance. This could have been because while the model used the refractive index of graphene, the experiments were carried out on a preparation of graphene oxide. Or this could have been the result of some light being reflected from the surface of the fluid resulting in less radiation reaching the sensor than was predicted by the model that did not consider surface effects.

3.2.2 Reflectance

To remove the effect of reflections from the experimental results and compare them to the simulated values the integrating sphere method was used on the Lambda 650 S UV/VIS to measure the reflectance of the samples. This also confirmed the assumption that scattering is low compared to absorption in the nanofluids investigated.

All the nanofluids samples had a lower reflectance value than the pure ethylene glycol. It was found that the reflectance decreased with increasing concentration of graphene oxide nanoparticles reaching a minimum at volume fraction of 0.012%. An increase in the volume fraction beyond 0.012% resulted into a rise in the reflectance as can be seen from Fig. 8. This optimum volume fraction of 0.012% for minimum reflectance is only valid for the pair of the specific nanoparticle (graphene oxide) and the ethylene glycol used in this study. In practice, even a slight change in the geometry and/or surface characteristics of the nanoparticles should alter this minimal volume fraction significantly.

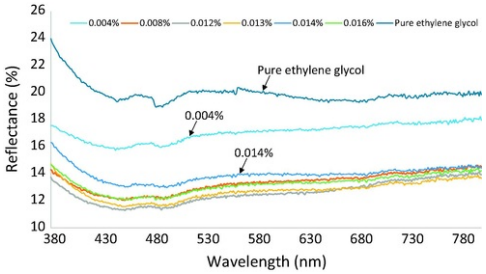

Fig. 8 Reflectance spectrum for different volume fractions.

3.2.3 Stability

The stability of ethylene glycol graphene oxide nanofluid was assessed by leaving the 0.008% sample undisturbed in the UV/VIS Spectrometer for 24 h. The sample's absorption was measured after 1, 2, 3 and 24 h. The change in absorbance measured over the 24-h time period was negligible as seen from Fig. 9 indicating that the fluid remained stable throughout the investigation.

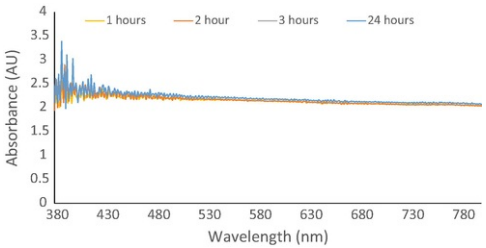

Fig. 9 Stability of nanofluid containing ethylene glycol and 0.008% graphene oxide.

4 Conclusions

The concept of using a wave optics model for the absorption of visible solar radiation (380–800 nm) by nanofluids was investigated. It is anticipated that such an approach would allow the suitability of a nanofluid for use in a volumetrically absorbing receiver of a concentrating solar collector to be assessed without the need for extensive laboratory tests on each candidate nanofluid. It was shown that even a relatively crude model, covering a control volume with depth only ten times the largest wavelength of 800 nm, could predict the solar absorbance of a nanofluid within 1AU of the trends seen in experimental data. In order to keep the cost of nanofluid low, an optimum volume fraction of 0.012% of graphene oxide is proposed to achieve a minimum reflectance and a sufficiently high absorption for a receiver of 10 mm diameter over the visible spectral range for a solar concentrator with a concentration ratio of 25. This optimum proportion is valid for the graphene oxide-ethylene glycol studied here. The model more accurately predicted the absorbance of the higher volume fraction samples than the lower ones. It is anticipated that a larger control volume will allow lower volume fractions to be simulated directly and so improve the accuracy of the model.

The model was dependant on measurements of refractive index or electrical permittivity of nanometre scale materials as such data is not readily available in peer reviewed public domain. The refractive index of graphene was used in the model to produce predictions that were compared to experimental data gathered on graphene oxide, another potential source of uncertainty in the results. It is hoped that more research into the properties of nano scale materials will widen the scope and improve the accuracy of wave optics models. Until such data is more widely available, models like the one presented here could reduce the number of laboratory tests needed to select a nanofluid for directly absorbing solar thermal applications as from only one test of the refractive index of a nanoparticle, the properties of those particles in any fluid can be predicted.

~~5 Uncited references~~

~~Berg et al. (2008), Hill and Jennings (1993), Jain et al. (2006), Kong and Cha (1996), Kottmann et al. (2000), Lance et al. (2003), Leen et al. (2009), Parameshwaran et al. (2013).~~

Acknowledgements

Authors, Rose, Singh, Tassou, Suresh and Anathraman, thankfully acknowledge the UKIERI-DST grant (IND/CONT/E/14-15/381) which made this research possible.

References

Berg M.J., Sorensen C.M. and Chakrabarti A., Extinction and the optical theorem. Part I. Single particles, *JOSA A* **25** (7), 2008, 1504–1513.

Bohren C.F. and Huffman D.R., Absorption and Scattering of Light by Small Particles, 1983, John Wiley & Sons.

Gorji T.B. and Ranjbar A.A., Geometry optimization of a nanofluid-based direct absorption solar collector using response surface methodology, *Sol. Energy* **122**, 2015, 314–325.

Hill J.M. and Jennings M.J., Formulation of model equations for heating by microwave radiation, *Appl. Math. Model.* **17** (7), 1993, 369–379.

Jain P.K., Kyeong S.L., Ivan H. and El-Sayed M.A., Calculated absorption and scattering properties of gold nanoparticles of different size, shape, and composition: applications in biological imaging and biomedicine, *J. Phys. Chem. B* **110** (14), 2006, 7238–7248.

Kerker M.P., McNulty P.J., Sculley M., Chew H. and Cooke D.D., Raman and fluorescent scattering by molecules embedded in small particles: numerical results for incoherent optical processes, *JOSA* **68** (12), 1978, 1676–1686.

Kong Y. and Cha C.Y., Reduction of NOx adsorbed on char with microwave energy, *Carbon* **34** (8), 1996, 1035–1040.

Kottmann J., Olivier M., Smith D. and Schultz S., Spectral response of plasmon resonant nanoparticles with a non-regular shape, *Opt. Express* **6** (11), 2000, 213–219.

Ladjevardi S.M., Asnaghi A., Izadkhast P.S. and Kashani A.H., Applicability of graphite nanofluids in direct solar energy absorption, *Sol. Energy* **94**, 2013, 327–334.

Lance K.K., Coronado E., Zhao L. and Schatz G.C., The optical properties of metal nanoparticles: the influence of size, shape, and dielectric environment, *J. Phys. Chem. B* **107** (3), 2003, 668–677.

Leen K.A., Bao K., Khan I., Smith W.E., Kothleitner G., Nordlander P., Maier S.A. and McComb D.W., Electron energy-loss spectroscopy (EELS) of surface plasmons in single silver nanoparticles and dimers: influence of beam damage and mapping of dark modes, *ACS Nano* **3** (10), 2009, 3015–3022.

Maikala R.V., Modified Beer's Law – historical perspectives and relevance in near-infrared monitoring of optical properties of human tissue, *Int. J. Ind. Ergon.* **40**, 2010, 125–134.

Ni Z.H., Wang H.M., Kasim J., Fan H.M., Yu T., Wu Y.H., Feng Y.P. and Shen Z.X., Graphene thickness determination using reflection and contrast spectroscopy, *Nano Lett.* **7** (9), 2007, 2758–2763.

Novotny L. and Hecht B., Principles of Nano-Optics, 2006, Cambridge University Press.

Otanicar T.P., Phelan P.E. and Golden J.S., Optical properties of liquids for direct absorption solar thermal energy systems, *Sol. Energy* **83** (7), 2009, 969–977.

Palik E.D., *Handbook of Optical Constants of Solids* **vol. 3**, 1998, Academic Press.

Parameshwaran R., Jayavel R. and Kalaiselvam S., Study on thermal properties of organic ester phase-change material embedded with silver nanoparticles, *J. Therm. Anal. Calorim.* **114** (2), 2013, 845–858.

Peatross J. and Ware M., Physics of Light and Optics, 2011, Brigham Young University, Department of Physics, 101–119.

Podolskiy V.A., Sarychev A.K. and Shalaev V.M., Plasmon modes in metal nanowires and left-handed materials, *J. Nonlin. Opt. Phys. Mater.* **11** (1), 2002, 65–74.

Romasanta L.J., Hernández M., López-Manchado M.A. and Verdejo R., Functionalised graphene sheets as effective high dielectric constant fillers, *Nanoscale Res. Lett.* **6** (1), 2011, 1–6.

Taylor R.A., Phelan P.E., Otanicar T.P., Adrian R. and Prasher R., Nanofluid optical property characterization: towards efficient direct absorption solar collectors, *Nanoscale Res. Lett.* **6** (1), 2011, 1–11.

Toppin-Hector A. and Singh H., Development of a nano-heat transfer fluid cooled direct absorbing receiver for concentrating solar collectors, *Int. J. Low Carbon Technol.* 2013, 1–6.

Highlights

- Different modelling approaches for the direct absorption of solar radiation by nanofluids discussed and evaluated.

- A wave optics model proposed for direct solar absorbing nanofluids.
- The wave optics model constructed and the results analysed.
- The optical properties of graphene oxide-ethylene glycol nanofluids characterised experimentally.
- The experimental results compared to those predicted by the model.

Queries and Answers

Query: Your article is registered as a regular item and is being processed for inclusion in a regular issue of the journal. If this is NOT correct and your article belongs to a Special Issue/Collection please contact s.sankaran@elsevier.com immediately prior to returning your corrections.
Answer: Yes its a regular item.

Query: The author names have been tagged as given names and surnames (surnames are highlighted in teal color). Please confirm if they have been identified correctly.
Answer: Yes they are correctly shown

Query: The citations “Novotny (2006) and Bohen (1983)” have been changed to match the author name/date in the reference list. Please check here and in subsequent occurrences, and correct if necessary.
Answer: Yes

Query: Reference “Koh et al. (2009)” is cited in the text but not provided in the reference list. Please provide it/them in the reference list or delete these citations from the text.
Answer: Deleted from the text as it was not required.

Query: This section comprises references that occur in the reference list but not in the body of the text. Please position each reference in the text or, alternatively, delete it. Any reference not dealt with will be retained in this section.
Answer: I have deleted these reference as these are not required.